Computers chem. Engng, Vol. 13, No. 8, pp. 881–898, 1989
Printed in Great Britain.

0098-1354/89 $3.00 + 0.00

CONVOLUTION AND DECONVOLUTION OF NONIDEAL TRACER RESPONSE DATA WITH APPLICATION TO THREE-PHASE PACKED-BEDS

P. L. MILLS† and M. P. DUDUKOVIĆ

Washington University Department of Chemical Engineering, 1 Brookings Drive, Campus Box 1198, St Louis, MO 63130-4899, U.S.A.

(*Received* 19 *January* 1988; *final revision received* 28 *December* 1988; *received for publication* 18 *January* 1989)

Abstract—Two methods are presented for evaluation of model parameters from nonideal tracer responses that represent convolution of the unit impulse response of the system under investigation and the response of other components. Both methods rely on time domain matching of experimental and model predicted curves. The first one relies on obtaining the unit impulse response of the system by deconvolution from the overall response. This method does not require an *a priori* model for the system, but its numerical implementation is possible only when an appropriate filter is used to reduce random noise which is present in the data to acceptable levels. Parameters are estimated by matching the deconvoluted unit impulse response to the model predicted one. Application of the fast Fourier transform and proper selection of regularization parameters in the implementation of this method are also described. The second method convolutes the model unit response with the response of other components to obtain the overall system response. Parameters are estimated by matching the overall system response to the experimental one. Interpretation of nonideal pulse tracer response data from a laboratory trickle-bed reactor is also performed to illustrate both methods.

INTRODUCTION

Dynamic tracer response methods are often used by chemical engineers for quantitative evaluation of transport and kinetic parameters in chemical and catalytic reactors as well as in other types of flow vessels. Some examples of the diverse reactor types where tracers have been used for such purposes include gas–solid fixed-beds (Schneider and Smith, 1968a, b; Suzuki and Smith, 1971), liquid–solid slurry reactors (Furusawa and Smith, 1973a, b, 1974; Furusawa and Suzuki, 1975), gas–liquid–solid slurry reactors (Niyama and Smith, 1976; Ramachandran and Smith, 1977, 1978a, b), trickle-bed reactors (Colombo *et al.*, 1976; Eroglu and Dogu, 1983; Kan and Greenfield, 1983; Mills *et al.*, 1979; Mills and Duduković, 1981; Ramachandran and Smith, 1979; Schwartz *et al.*, 1976; Sicardi *et al.*, 1980; Van Swaaij *et al.*, 1969), gas–solid single-pellet devices (Dogu and Smith, 1975; Dogu *et al.*, 1986; Waldram *et al.*, 1988) and gas–solid fluidized-beds (Pamuk and Dogu, 1978). Numerous other examples of tracer applications in the various engineering disciplines, catalysis and medical applications, to name a few, have been summarized in assorted reviews and monographs on the subject (Duduković, 1986; Fahim and Wakao, 1982; Kobayashi and Kobayashi, 1974; Furusawa *et al.*, 1976; Nauman and Buffham, 1983; Pehtö and Noble, 1982; Ramachandran and Smith, 1978b) Ramachandran and Chaudhari, 1983; Wen and Fan, 1975). Thus, tracer testing and the information derived from it has been considered quite useful in a number of applied science areas.

An integral part of successful tracer testing involves interpretation of the tracer response data. Some limited information, such as fluid holdups and partition coefficients, can be obtained from tracer data without the use of a flow model by application of the central volume principle (Duduković, 1986; Nauman and Buffham, 1983). However, the real utility of tracer testing occurs when a flow model is developed to describe the physicochemical processes, and the model parameters are determined from the experimental tracer data using parameter estimation techniques (Seinfeld and Lapidus, 1974). The preferred model is one that matches the data with the smallest error, yet described the physics with the smallest number of realistic parameters. Various factors associated with model building have been summarized elsewhere (Nauman and Buffham, 1983; Seinfeld and Lapidus, 1974; Shinnar, 1978; Wen and Fan, 1975).

Techniques for determination of model parameters in tracer flow models using experimental tracer response data include the method of moments (Aris, 1959; Bischoff, 1960; Colombo *et al.*, 1976; Dogu and Smith, 1975; Dogu *et al.*, 1986; Eroglu and Dogu, 1983; Furusawa and Smith, 1973a, b, 1974; Furusawa and Suzuki, 1975; Mills *et al.*, 1979; Mills and Duduković, 1981; Niyama and Smith, 1976; Pamuk and Dogu, 1978; Schneider and Smith, 1968a, b; Schwartz *et al.*, 1976; Suzuki and Smith, 1971; Van Swaaij *et al.*, 1969; Wakao and Tanaka, 1973), the

†Author to whom all correspondence should be addressed.

method of weighted moments (Anderssen and White, 1977; Michelsen and Ostergaard, 1970; Mixon *et al.*, 1967; Ostergaard and Michelsen, 1969; Wolff *et al.*, 1979; 1980), Laplace and Fourier transform domain analysis (Anderssen and White, 1970; Chou and Hegedus, 1977; Clements, 1969; Felder *et al.*, 1974; Gangwal *et al.*, 1971; Gosset, 1974; Harrison *et al.*, 1974; Haynes, 1978; Hays *et al.*, 1967; Michelsen and Ostergaard, 1970; Ostergaard and Michelsen, 1969; Rajakumar and Krishnaswamy, 1975; Ramachandran *et al.*, 1986) and time-domain parameter estimation (Boersma-Klein and Moulijn, 1979; Fu, 1970; Lee *et al.*, 1981; Michelsen, 1972; Sicardi *et al.*, 1980; Wakao and Tanaka, 1973; Wakao *et al.*, 1978, 1980). The governing relationships for each of these methods are given in the various references cited above, in assorted monographs (Nauman and Buffham, 1983; Pehtö and Noble, 1982; Ramachandran and Chaudhari, 1983; Seinfeld and Lapidus, 1974; Wen and Fan, 1975) and review papers (Duduković, 1986; Fahim and Wakao, 1982; Ramachandran and Smith, 1978a, b; Weinstein and Duduković, 1975) so that these will not be described here. A key conclusion obtained from these independent sources is that time-domain analysis of tracer response data is the preferred technique for discrimination between various flow models and for flow model parameter estimation. However, time-domain analysis is more difficult to implement which explains why the method of moments, despite its notable drawbacks (Radeke, 1981), continues to be used (cf. Dogu, 1986; Van Zee *et al.*, 1987). A general approach for performing time-domain analysis of tracer response data for linear systems which can be implemented on available computers using modern and efficient mathematical methods would appear to fill an existing gap in this area.

The primary objective of this work is to present two independent computer-based methods for time-domain analysis of nonideal pulse tracer response data that are based upon the concepts of convolution and deconvolution (Baker, 1977; Blass and Halsey, 1981; de Hoog, 1980; Jakeman and Young, 1980; Jansson, 1984; Ziolkowski, 1984). The latter one is not widely employed in chemical engineering applications, although it is mentioned in one of the standard textbooks in chemical reaction engineering (Levenspiel, 1972) and has been recognized as a formidable problem in a few recent publications (Duduković, 1986; Van Zee *et al.*, 1987) on tracer applications. Another objective is to present computer algorithms that implement the convolution and deconvolution methods, and to illustrate their usage by application to tracer response data obtained from a laboratory-scale trickle-bed reactor. A final objective is to compare the results obtained by each method and to point out their limitations where applicable.

The convolution and deconvolution techniques presented here provide two independent means of flow model discrimination and parameter estimation. In both cases, it is assumed that the experimental tracer response data have been cast into normalized form to yield the input forcing function $x(t)$ and system output response $y(t)$. The function $x(t)$ represents the tracer response of the nonideal tracer injection and sampling system which, in an ideal system, is described by the Dirac delta function $x(t) = \delta(t)$. In the case of deconvolution, the impulse response of the reactor or test section $E(t)$ is first determined by inversion of the convolution integral operator using $x(t)$ and $y(t)$. The vector of model parameters $\bar{P}$ that appear on the impulse response of an assumed flow model $E(t, \bar{P})$ are then obtained by minimization of a suitable least squares objective function. In the case of convolution, the impulse response of an assumed flow model is convoluted with the forcing function $x(t)$ to obtain a model predicted output response $y_p(t, \bar{P})$. The model parameters are determined using the same approach described above for deconvolution, except the objective function is based upon an error criterion that uses the model-predicted output response $y_p(t, \bar{P})$ and experimental output response $y(t)$.

This paper presents the methodology for systematic application of the above two procedures while reducing the inherent errors and addresses the question as to which method should be preferred.

EXPERIMENTAL PRELIMINARIES

Before presenting the details of the convolution and deconvolution methods, it is instructive to describe typical tracer experiments for which the proposed methods can be utilized. A specific example will be given in a later section. The setting is assumed to be one where one or more phases, such as gas and liquid, are metered at known flowrates to a chemical reactor or other test section. Upstream of the reactor, an appropriate valving arrangement is used to introduce a quantity of tracer at some prescribed time $t = 0$ into one of the flowing phases where it is introduced to the reactor. Downstream of the reactor, the tracer concentration, or some quantity that is linearly related to the tracer concentration (e.g. voltage), is measured with an appropriate sensor or detector to give a discrete data record for the impulse response of the system $Y(j\Delta t)$ where $j = 0, 1, \ldots, N-1$ is the sample number and Δt is the sampling interval. The test section is then removed, the inlet and exit lines used for transport of the flowing phase are connected without addition of any significant external system volume, and the experiment is repeated at the same conditions (flowrate, tracer concentration, etc.). The resulting data record corresponds to the impulse response of the combined injection-sampling system and detector $X(j\Delta t)$. Figure 1 compares hypothetical tracer responses that would be obtained from such an experiment for both an ideal (Fig. 1a) and a nonideal (Fig. 1b) test system. For the ideal system, the response of all system

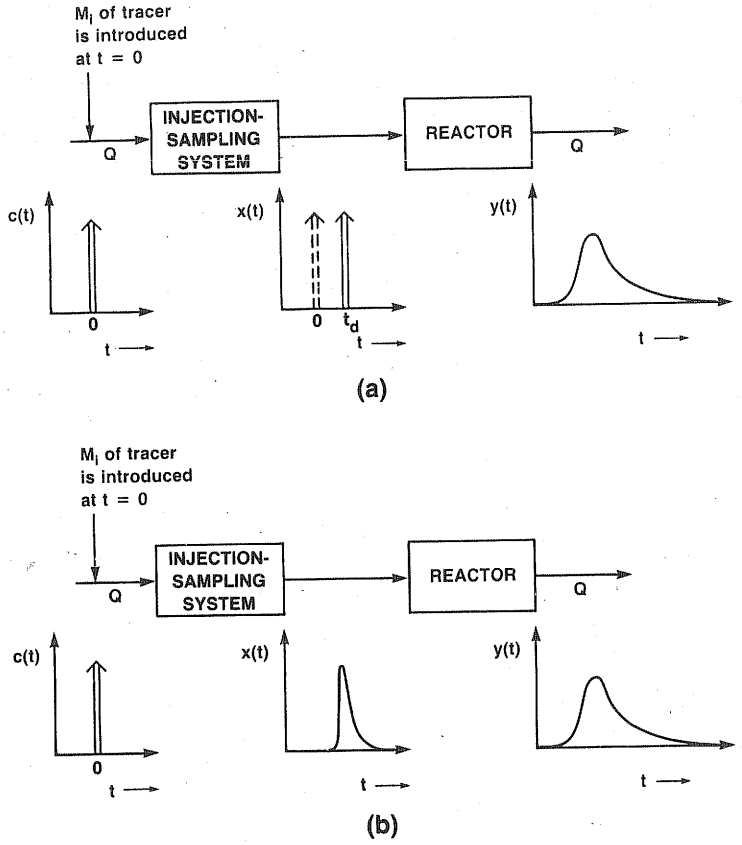

Fig. 1. Comparison of tracer impulse responses for systems having an ideal injection-sampling system (a) and a nonideal injection-sampling system (b).

components that are external to the reactor correspond to plug-flow with a time delay, i.e. $x(t) = \delta(t - t_d)$. The nonideal system exhibits a response $x(t)$ which deviates from plug flow so that a simple delta function does not accurately describe the response. Most practical tracer tests are of the latter type so that proper time-domain interpretation of the output response $y(t)$ must account for the nonideal nature of the input $x(t)$.

The experiment described above represents only one example where the methods presented below can be applied. In many cases, such as in commercial systems, it is often not feasible to measure the response of the injection-sampling system $X(j\Delta t)$ due to physical restrictions. A reasonable flow model whose parameters can be calculated from first principles or existing correlations should then be used to provide approximate values for the normalized input response x_j. This can then be used in conjuction with experimental values for the overall system output response $Y(j\Delta t)$ for subsequent data reduction and interpretation.

Another situation of interest is the case where a tracer input is introduced into a system and the response is simultaneously measured downstream of the injection point at two different locations using probes or other sensors. A typical example is given in Levenspiel (1972) and more recently by Van Zee *et al.* (1987). The responses at the upstream and downstream locations would then correspond to $X(j\Delta t)$ and $Y(j\Delta t)$, respectively. Interpretation of the flow processes between these two points using these responses would be one of the objectives.

Additional details on correct experimental procedures for conducting tracer tests, reduction of the raw experimental data and evaluation of the various tracer probability density functions are given elsewhere (Dudukovic, 1986; Nauman and Buffham, 1983). Use of the time-domain data interpretation methods outlined below will be worth doing only if these preliminary steps have been properly followed so that the data can be considered reliable.

DECONVOLUTION METHOD

Deconvolution of nonideal input–output tracer response data, such as that shown earlier in Fig. 1b, to obtain the normalized impulse response of the test section (chemical reactor, etc.) is described below. The numerical difficulties associated with using conventional approaches are outlined first. This is then followed by the recommended method based upon discrete Fourier transforms with signal filtering.

Matrix solution

If the normalized input–output tracer responses (Duduković, 1986) are denoted by x_j and y_j and the system is linear, i.e. the principle of superposition can be experimentally verified, then the impulse response of the test section e_j is related to x_j and y_j by the discrete periodic convolution:

$$y_k = z_k + \epsilon_k = \sum_{j=0}^{N-1} x_{k-j} e_j, \qquad k = 0, 1, \ldots, N-1. \tag{1}$$

In equation (1), the normalized responses x_j and y_j have been periodically extended with the period N, i.e. their indices are calculated as modulo N so that $x_{j+mN} = x_j$ for any integer m, and similarly for e_j and y_k. Measurement errors and random noise that are present in the data, which can be associated with the given tracer detection equipment, or which occur as a result of minor fluctuations in experimental variables, are denoted by ϵ_k. Although it might be possible to define limits on the magnitude of the errors ϵ_k, *a priori* assignment of these at each sampled point k is generally impossible. If these were known, the exact values for the sytem response would be given by $z_k = y_k - \epsilon_k$. Expansion of equation (1) gives:

$$\begin{bmatrix} y_0 \\ y_1 \\ \vdots \\ y_{N-2} \\ y_{N-1} \end{bmatrix} = \begin{bmatrix} x_0 & x_{N-1} & \cdots & x_2 & x_1 \\ x_1 & x_0 & \cdots & x_3 & x_2 \\ \vdots & \vdots & & \vdots & \\ x_{N-2} & x_{N-3} & & x_0 & x_{N-1} \\ x_{N-1} & x_{N-2} & & x_1 & x_0 \end{bmatrix} \begin{bmatrix} e_0 \\ e_1 \\ \vdots \\ e_{N-2} \\ e_{N-1} \end{bmatrix}. \tag{2}$$

The above system of linear equations, whose unknowns are the sampled values of the impulse response e_j, can be written in matrix form as

$$\bar{y} = \mathbb{x}\bar{e}. \tag{3}$$

Solving for the impulse response of the test from equation (3) gives:

$$\bar{e} = \mathbb{x}^{-1}\bar{y}. \tag{4}$$

Despite the apparent simplicity of equation (4) for deconvolution, it cannot be used in practical applications for several reasons. First, the sampling rates necessary to accurately define the tracer response curve may consist of hundreds, or even thousands of points. This makes the inversion of the dense matrix $\mathbb{x}$ impractical, or even impossible, even on the largest computers. Second, the matrix $\mathbb{x}$ is ill-conditioned (Baker, 1977; de Hoog, 1980; Jakeman and Young, 1980) so that small errors in the x_j can result in large perturbations when the matrix inverse $\mathbb{x}^{-1}$ is evaluated.

Unfiltered Fourier transform solution

The problems associated with the solution of equation (2) for the impulse response sequence e_j can be better appreciated by using Fourier transforms. Recall that the discrete Fourier transform (DFT) of a sampled complex function a_j for $j = 0, 1, \ldots, N-1$ is (Brigham, 1974):

$$A(n) = \frac{1}{N} \sum_{j=0}^{N-1} T a_j \exp\left[\frac{-2\pi i j n}{N}\right]; \qquad n = 0, 1, \ldots, N-1, \tag{5}$$

where $i = \sqrt{-1}$ and T is the sampling period. Equation (5) is the approximation obtained when the continuous function $a(t)$ is defined as a periodic function $a_p(t)$ over $(0, T)$ and trapezoidal quadrature with a spacing $\Delta t = T/N$ is applied, neglecting end corrections. Applying the DFT convolution theorem (Brigham, 1974) to equation (1) and solving for the DFT of the impulse response e_j gives:

$$E(n) = \frac{Z(n)}{X(n)} + \frac{B(n)}{X(n)} = \frac{Y(n)}{X(n)}, \tag{6}$$

where $X(n)$, $Z(n)$ and $B(n)$ are the DFTs of x_j, z_j and ϵ_k, respectively. While the ratio of Fourier transforms of the output–input $Z(n)/X(n)$ in equation (6) is well-behaved and stable for the class of linear systems encountered in normal pulse testing (Seinfeld and Lapidus, 1974; Wen and Fan, 1975), the corresponding ratio of DFTs for the error and input denoted by $B(n)/X(n)$ will be the dominant term. The end result is that the DFT of the impulse response $E(n)$ and the inverse e_j cannot be obtained using this simplistic approach since it is often obliterated by low to high frequency noise generated by the $B(n)/X(n)$ term. An example of the application of equation (6) to actual tracer response data will be given in a later section which illustrates this point.

Rather than using the DFT, which can be efficiently implemented by the fast Fourier transform (FFT) algorithm using various commercially-available software packages, some previous results given in chemical engineering literature (Boersma-Klein and Moulijn, 1979; Clements, 1969; Felder *et al.*, 1974; Gangwal *et al.*, 1971; Harrison *et al.*, 1974; Haynes, 1978; Hays *et al.*, 1967) have employed other quadrature rules and related approximations to evaluate the numerical Fourier transform. It has been suggested (Haynes, 1986) that the poor results obtained through application of equation (6) are due to the use of both the DFT and the FFT. Our experience in using these alternate methods have shown that the use of higher-order quadrature methods with smaller truncation errors exhibit behavior that are similar to

those for the DFT when tested on actual experimental data. This seems to agree with the recent results of another independent study (Watanabe and Himmelblau, 1986) where the operation defined by equation (6) leads to apparently unacceptable results.

Fourier transform solution with filtering

The problems associated with solution of the numerically unstable system of linear equations defined by equation (1) has resulted in numerous investigations in applied mathematics literature on development of stable deconvolution methods. Many of these have been classified according to a particular methodology and summarized in several monographs on integral equations and deconvolution methods (Baker, 1977; Blass and Halsey, 1981; Jakeman and Young, 1980; Jansson, 1984; Ziolkowski, 1984). A review of these suggests that those which involve the use of biased estimators or digital filters are preferred for analysis of tracer data since they can be efficiently implemented using the fast Fourier transform which avoids the difficulties associated with inversion of large, ill-conditioned matrices. A particularly useful method was first proposed by Phillips (1962) and later extended by Twomey (1965) and is based upon the method of regularization. In this method, an approximate solution to equation (3) for the impulse response, say $\bar{e}_a$, is sought such that the residual $\bar{r} = \mathbb{x}\bar{e} - \bar{y}$ is minimized in a least-squares sense subject to the constraint that the solution $\bar{e}_a$ satisfies an nth order smoothness formula. Formally, this results in the following objective function when the Lagrangian multiplier method is used (Hunt, 1970, 1971) for incorporation of the constraint:

$$\phi(\bar{e}_a) = (\mathbb{x}\bar{e}_a - \bar{y})^T(\mathbb{x}\bar{e}_a - \bar{y}) + \gamma(\mathbb{C}\bar{e}_a)^T(\mathbb{C}\bar{e}_a), \quad (7)$$

where T denotes the matrix transpose. The matrix $\mathbb{C}$ in equation (7) is formed, if second-order smoothness is desired, by convolution with the sequence $(-1, 2, 1)$ and its associated convolution matrix. The reciprocal of γ, i.e. γ^{-1}, represents the Lagrangian multiplier. Minimization of equation (7) with respect to $\bar{e}_a$ leads to the following expression (Hunt, 1971) for the impulse response from experimental input–output tracer response data:

$$\bar{e}_a = (\mathbb{x}^T\mathbb{x} + \gamma\mathbb{C}\mathbb{C}^T)^{-1}\mathbb{x}\bar{y}. \quad (8)$$

By considering the properties of the various matrices and making appropriate assumptions regarding the matrix $\mathbb{C}$ in equation (8), Hunt (1970) showed that equation (8) can be cast into an equivalent form in terms of discrete Fourier transforms. The details of this derivation are lengthy and are omitted here for brevity. The final working relationship for the DFT of the impulse response is:

$$E_a(n) = \frac{Y(n)/X(n)}{1 + \gamma \dfrac{C(n)C^*(n)}{X(n)X^*(n)}}, \quad (9)$$

where $X(n)$, $Y(n)$ and $C(n)$ are the DFTs of the normalized experimental input response x_j, output response y_j, and smoothing formula coefficients c_j, respectively, which are obtained using equation (5). The quantities marked with an asterisk denote the complex conjugate.

Inspection of equation (9) shows that the term $\gamma C(n)C^*(n)/X(n)X^*(n)$ is present which has the form of a digital filter. This removes measurement errors and noise from the data in an amount that depends primarily upon the assumed magnitude of the filtering parameter γ. If this parameter can be properly selected, then an approximation to the time-domain impulse response can be obtained from equation (9) using the inverse discrete Fourier transform (IDFT):

$$e_{a,j} = \frac{1}{T}\sum_{n=0}^{\infty} E_a(n) \exp\left[\frac{2\pi ijn}{N}\right], \quad j = 0, 1, 2, \ldots, N-1. \quad (10)$$

Selection of the filtering parameter γ

Inspection of equation (9) shows that the DFT of the impulse response $E_a(n)$ has an infinite number of solutions since the filtering parameter γ is unbounded in $(0, \infty)$. In the limit as $\gamma \to 0$, it reduces to equation (6), i.e. $E_a(n) = Y(n)/X(n)$, which is the DFT of the impulse response without filtering of the measurement errors and noise. In the limit as $\gamma \to \infty$, then $E_a(n) = 0$ which is an unacceptable solution based on physical grounds. These two limits suggest that a proper choice of the filtering parameter γ will remove the frequency components of the errors so that $E_a(n)$ is well-behaved while preventing oversmoothing so that the essential frequency components of the solution are not deleted. As pointed out in applied mathematics literature (Baker, 1977; de Hoog, 1980; Jakeman and Young, 1980), regularization methods have the drawback of requiring the user to specify some technique for determining γ.

The technique used here to identify the filtering parameter γ employs the additivity property for the moments of the normalized tracer impulse responses (Levenspiel, 1972). From the normalized tracer data for the input–output responses x_j and y_j, respectively, one must first evaluate the nth absolute moments for the normalized impulse response of the test section denoted here by $\mu_{n,r}$ according to:

$$\mu_{n,r} = \mu_{n,y} - \mu_{n,x}, \quad (11)$$

where the nth absolute moment of the injection-sampling system response is:

$$\mu_{n,x} = \int_0^{\infty} t^n x(t)\, dt. \quad (12)$$

The nth absolute moment of the system output response $\mu_{n,y}$ is defined by replacing $x(t)$ with $y(t)$ in equation (12). Numerical evaluation of these moment relations is performed by Simpson's one-third rule or

a similar quadrature rule for $0 \leqslant t \leqslant t^*$, while the contribution for $t^* \leqslant t \leqslant \infty$ is obtained by fitting the tail to a single exponential decay with closed-form evaluation of the resulting integral. Additional details on this aspect are given by Duduković (1986).

As described in the previous section, deconvolution of the input–output tracer response data for an assumed value of γ yields an approximation to the impulse response of the test section according to equation (10), i.e. $e_j \cong e_{a,j}$. Numerical evaluation of equation (12) with $x(t)$ replaced by $e_{a,j}$ yields independent values for the nth absolute moments of the test section, say $\mu'_{n,r}$. The appropriate value of the filtering parameter γ has been chosen when these moments differ by those obtained from equation (11) within a certain prescribed error. The problem then becomes one of determining the value of γ such that:

$$\sum_{n=0}^{n\max} |1 - \mu'_{n,r}/\mu_{n,r}|^2 \leqslant \epsilon, \tag{13}$$

where ϵ is a prescribed error criterion and $n\max$ is the maximum order of the absolute moment, e.g. $n\max = 2$. For a given value of ϵ, γ can be determined by any suitable root-finding technique, such as Wegstein's method.

A few comments are in order regarding the method outlined above for identifying the filtering parameter γ. Since *a priori* estimates of γ are not available, it becomes necessary to use an arbitrarily selected value to initiate the iteration process. In our experience, the use of interactive computer graphics that plots both the Fourier transform and time-domain impulse responses along with the normalized input and output responses is recommended. This allows the user to decide whether or not the initial and subsequent values of γ lead to deconvoluted responses which agree with common sense judgment. For example, the impulse response should have features that represent, more or less, a weighted average of the input and output responses. In addition, depending on the relative accuracy of the tails of the input–output tracer responses, one may also decide that only the zeroth and first absolute moments should be used for the determination of γ from equation (13).

As mentioned earlier, the solution of the convolution integral equation is well-known as being an ill-posed problem, especially when the forcing function $x(t)$ and output response $y(t)$ are based upon experimental measurements which contain random errors. Thus, precise specification of γ is not realistic and usually a range of values can be identified which will give acceptable results. In practice, a value of γ should be selected so that the moments of the impulse response satisfy equation (11) for $0 \leqslant n \leqslant 2$. Evaluation of the third and higher moments for pulse responses is usually not reliable (Radeke, 1981) and is not recommended for determination of γ.

Once the proper value for the filtering parameter has been identified using the method outlined above, the user can also obtain an estimate of the mean-squared error (MSE) or residual between the approximate solution for the impulse response $\bar{e}_a$ and the exact solution $\bar{e}$. It can be shown that the MSE is given by (Hunt, 1971):

$$\text{MSE} = \sum_{k=0}^{N} \epsilon_k^2 \cong N \sum_{n=0}^{N-1} \frac{Y(n)Y^*(n)}{\left[1 + \gamma^{-1} \dfrac{X(n)X^*(n)}{C(n)C^*(n)}\right]^2}. \tag{14}$$

This involves a straightforward finite summation of discrete Fourier transforms that are already available from the previous steps of the calculation. If an estimate of the MSE can be made, then application of a 1-D root finding method to equation (14) will permit an *a priori* estimate of the filtering parameter γ.

CONVOLUTION METHOD

An alternate approach for time-domain analysis of tracer response data is based upon convolution. This method avoids the numerical instabilities associated with deconvolution since inversion of the ill-conditioned convolution operator through matrix operations, or through division of discrete Fourier transforms, is avoided.

The key starting relationships have already been set forth in the previous section so that only a few additional ones are needed. As in the case of deconvolution, normalized tracer response data for the injection-sampling system x_j (input) and for the combined injection-sampling system and test section y_j (output) are assumed to be available. If a particular linear flow model that describes the tracer transport processes is assumed, then a closed-form expression for the model-predicted impulse response in the Laplace transform domain $\bar{E}(s, \bar{P})$ can usually be obtained where s is the transform variable and $\bar{P}$ is the vector of model parameters. If the DFT convolution theorem (Brigham, 1974) is applied, then the model-predicted output response in the Fourier transform domain will be:

$$Y_p(n, \bar{P}) = \bar{E}(n, \bar{P})^* X(n), \qquad n = 0, 1, \ldots, N-1. \tag{15}$$

where $X(n) = \text{DFT}(x_j)$ as defined earlier by equation (5) and $i = \sqrt{-1}$. In the above equation, the shorthand notation $\bar{E}(n, \bar{P}) = \bar{E}(s = 2\pi \text{ in}/N, \bar{P})$ has been used to denote the DFT of the model-predicted response. In practice, this is obtained by substituting $s = i\omega$ in $\bar{E}(s, \bar{P})$ and identifying the real and imaginary parts of $\bar{E}(i\omega, \bar{P}) = \bar{E}_r(i\omega, \bar{P}) + i\bar{E}_i(i\omega, \bar{P})$. These are then sampled at the discrete frequency values $\omega_n = 2\pi n/N$ for $n = 0, 1, \ldots, N-1$ to form the complex form of $\bar{E}(n, \bar{P})$. Despite the presence of measurement errors and noise in the x_j, these are not amplified when the DFT is taken and the multiplication of two complex numbers, namely $X(n)$ and $\bar{E}(n, P)$, is performed as indicated above by equation (15).

The model predicted output response in the time-domain is readily obtained by applying the IDFT defined by equation (10) to $Y_p(n, \bar{P})$ given above. Thus:

$$y_{p,j} = \text{IDFT}[Y_p(n, \bar{P}) \qquad j = 0, 1, \ldots, N-1. \tag{16}$$

PARAMETER ESTIMATION

The utility of both the convolution and deconvolution methods is that the parameters in one or more linear flow models can be obtained by parameter estimation techniques. The methods used in the example given later are summarized below.

Deconvolution method

A major difference between the convolution and deconvolution methods is that the latter one does not require an assumed linear flow model to obtain the impulse response of the test section since this response is produced directly from the input–output data. In certain applications, development of a linear flow model that describes the tracer transport may not be an important objective and only the experimental impulse response of the test section may be needed. For cases where parameters are desired, however, the following objective function based upon the squared relative errors between the model-predicted and experimental impulse responses in the time-domain can be defined:

$$\phi_d = \sum_{j=0}^{N-1} w_j \left[\frac{e_{p,j} - e_{a,j}}{e_{a,j}}\right]^2. \tag{17}$$

In this equation, values for the experimental impulse response $e_{a,j}$ are the ones obtained from equation (10) using the deconvolution method with filtering. Time-domain values for the model-predicted impulse response can be obtained from either a closed-form expression for $E(t, \bar{P})$ or by numerical inversion of the Laplace-transformed impulse response $\bar{E}(s, \bar{P})$. The results given here are based upon the latter approach using the following Laplace transform inversion formula (Crump, 1976):

$$e_{p,j} = \frac{e^{bt}}{T}\left[\frac{1}{2}\bar{E}(a, \bar{P}) + \sum_{k=1}^{\infty} \text{Re}\left\{\bar{E}\left(b + \frac{k\pi i}{T}, \bar{P}\right)\right\} \cos\frac{k\pi t_j}{T} - \sum_{k=1}^{\infty} \text{Im}\left\{\bar{E}\left(b + \frac{k\pi i}{T}, \bar{P}\right)\right\} \sin\frac{k\pi t_j}{T}\right] + \text{error}. \tag{18}$$

The approximation error in the numerical inverse is:

$$\text{error} \leq \frac{Me^{bt}}{e^{2T(b-\beta)} - 1}, \quad 0 < t < 2T \tag{19}$$

where it is assumed that $|E(t, \bar{P})| \leq Me^{\beta t}$. The parameter β is chosen such that $\beta \geq \max\{\text{Re}(x_i)\}$ where x_i is a pole of $\bar{E}(s, \bar{P})$. The parameter b is the real part of the Laplace transform parameter s and is selected so that:

$$b = \beta - \frac{\ln E_r}{2T}, \tag{20}$$

where E_r is an estimate of the rounding error. The parameter T is the sampling time period over which the model-predicted impulse response is desired. A computer program that implements equation (18) is available in the IMSL library (1982).

Convolution method

The convolution method yields the model-predicted response in both the Fourier transform and the time-domain according to equations (15) and (16), respectively. Since the objective here is to perform a direct time-domain comparison of the normalized experimental output response y_j to the model-predicted response $y_{p,j}$, the following objective function for parameter estimation can be defined:

$$\phi_c = \sum_{j=0}^{N-1} w_j \left[\frac{y_{p,j} - y_j}{y_j}\right]^2. \tag{21}$$

Minimization of the above objective function, which is based upon the squared relative error, was performed in this work using Marquardt's method (Seinfeld and Lapidus, 1974). The weighting factors w_j were assigned to be unity corresponding to a uniform weighting of all data. Initial parameter estimates were obtained, in the case of two-parameter models, by comparison of the theoretical expressions for the moments (mean and variance) to those calculated from the data. For models having more than two parameters, two of the parameters were obtained using the above approach while the remaining ones (e.g. mass transfer coefficients, etc.) were estimated from literature correlations.

COMPUTER SOFTWARE

Computer software has been developed which implements the convolution and deconvolution methods described above in FORTRAN 77 on an IBM 3081. Calculated results are output to disk files where they are plotted using the ISSCO graphics package called DISSPLA on either an IBM 3179G terminal, or a HP 7550A 8-pen plotter. Evaluation of either the DFT or the IDFT according to equations (5) or (10), respectively is performed by a program that implements the base 2 FFT algorithm of Cooley and Tukey (Brigham, 1974) on the DFT. This same program, and others which are commercially available, can be used to evaluate the IDFT by appropriate modifications to the input and output data arrays. Details on this are available in standard reference texts on the subject (Brigham, 1974). Typical CPU times to perform deconvolution or convolution and parameter estimation for the four-parameter model given below were 10 s or less.

EXAMPLE APPLICATION

The methods described above for convolution and deconvolution have been applied to experimental tracer response data obtained in our laboratory from a trickle-bed reactor. A description of the experimental apparatus and procedure are available elsewhere (Mills and Duduković, 1981) to which the reader is referred for details. To briefly summarize, pulse tracer response measurements were performed under isothermal conditions at $T = 295$ K using a 1.35 cm i.d. × 40-cm long reactor containing granular nonporous alumina particles with an average particle dia 0.0718 cm. For the two-phase flow experiments reported here, He and n-hexane were used as the gas and liquid phases with superficial mass velocities of 0.15 and 0.12 kg m^{-2} – s^{-1}, respectively. These conditions correspond to the trickle-flow regime on the flow map of Charpentier and Favier (Ramachandran and Chaudhari, 1983). The tracer was n-pentane which had been shown in previous liquid-full tracer experiments to be nonadsorbing when the reduced data were compared to the expression for the first absolute moment from a dispersion type flow model that included tracer adsorption, mass transfer and diffusion (Mills and Duduković, 1981). By carefully connecting the tubing between the tracer injection valve and the reactor inlet with the tubing that connected the reactor exit with the refractive index detector, the tracer impulse response of the combined injection-sampling system could be obtained at a given liquid flowrate. The same tracer response experiments were then repeated with the reactor in place to obtain the responses of the overall system.

Figure 2 shows a typical set of normalized tracer responses obtained from the above experiments. A time sampling increment of $\Delta t = 2$ s was used for the combined injection-sampling system, while an increment of $\Delta t = 3$ s was used for the overall system. The

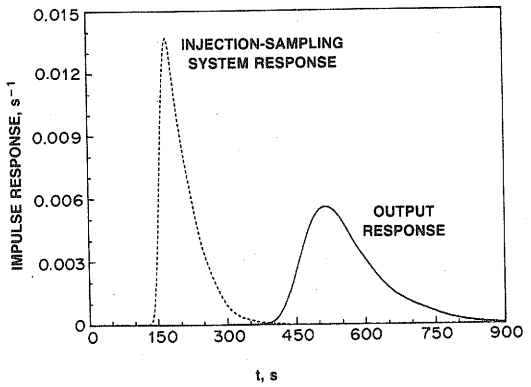

Fig. 2. Normalized tracer response data obtained from trickle-bed reactor experiments with nonporous packing. Parameters: $d_p = 7.18 \times 10^{-4}$ m, $d_t = 1.35 \times 10^{-2}$ m, $L_p = 0.4$ m, $L_m = 0.15$ kg m^{-2} s^{-1}, $G_m = 0.12$ kg m^{-2} s^{-1}, $T = 295$ K, liquid-phase = hexane, gas-phase = helium, tracer = pentane.

indicated values for the first absolute moment μ_1 and the variance $\sigma^2 = \mu_2 - (\mu_1)^2$ of the response curves are based upon evaluation of equation (12) as described in an earlier section. According to equation (11), the reactor impulse response $e(t)$ should have a first absolute moment of $\mu_{1,r} = 356$ s and a variance $\sigma_r^2 = 6113.7$ s^2. The tracer mass balance for both the input and output responses was satisfied within 0.4–0.6% when the total amount of tracer injected was compared to that determined from the zeroth moments and the measured value of the liquid volumetric flowrate.

Figure 3 shows typical results that are obtained when deconvolution of the input–output tracer responses given above in Fig. 2 is attempted using the conventional approach without filtering. According to this method, the reactor impulse response in the Fourier transform domain at a given frequency is simply the Fourier transform of the output response divided by the Fourier transform of the input response as defined by equation (6). Figures 3a and b show the real and imaginary parts of the Fourier-transformed input and output responses $X(n)$ and $Y(n)$, respectively. Both of these are smooth, damped functions that do not show any obvious presence of measurement errors and noise in the Fourier transform domain. The Fourier-transformed input response $X(n)$ has oscillations that approach zero at a larger value of frequency when compared to the Fourier-transformed output response $Y(n)$. Figure 3c shows that the quotient of these transforms $E(n) = Y(n)/Z(n)$ yields a reactor impulse response in the Fourier-transform domain that is highly irregular and does not approach a limiting value of zero with increasing values of frequency as expected. Instead, the magnitude of the oscillations appear to increase with increasing frequency values. As pointed out earlier below equation (6), the Fourier-transform of the reactor impulse response $E(n)$ is defined in terms of the sum of $Z(n)/X(n)$ and $B(n)/X(n)$ where $X(n)$, $Z(n)$ and $B(n)$ are the Fourier transforms of the input response, error-free output response and measurement error response, respectively. The results in Fig. 3c provide direct evidence that the ratio of $B(n)/X(n)$ is a significant factor in the reactor impulse response that must be reduced before reliable values of $E(n)$ can be obtained.

Having shown that the conventional method for deconvolution of tracer input–output responses fails to produce correct results for the reactor impulse response, application of the filtering method for deconvolution is now illustrated. Figures 4a–c show the effect of the smoothing parameter γ on the reactor impulse response in the Fourier-transform domain. In this case, the real and imaginary parts of the response were obtained from equation (9), assuming $C(n) = \text{DFT}\ [1, -2, 1, 0, \ldots]$ corresponding to a second-order smoothing formula. Numerical experiments using first-order, third-order and fourth-order smoothing formulae produced values for $E_a(n)$ that

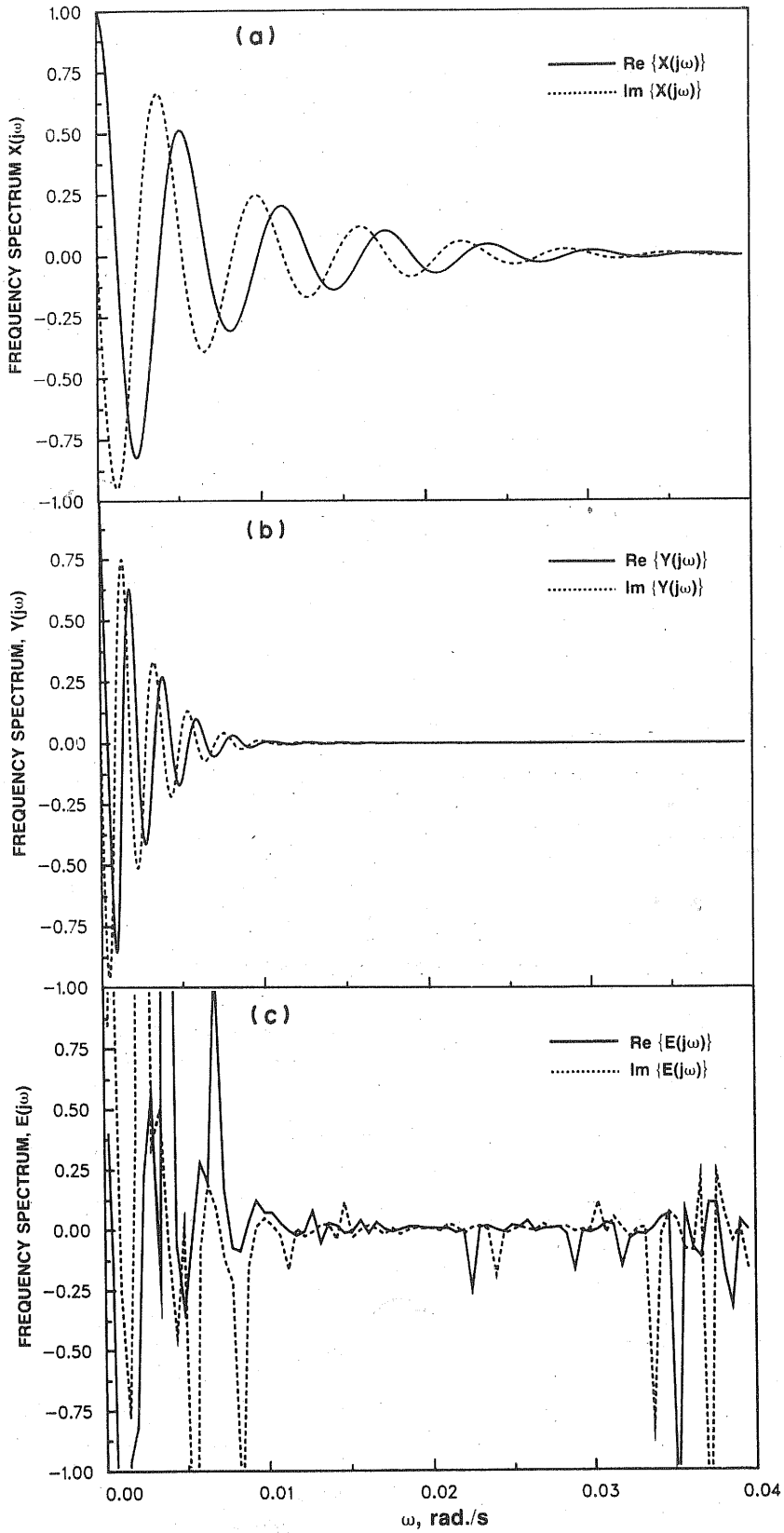

Fig. 3. Fourier transforms of the normalized tracer responses: (a) input response $X(j\omega)$; (b) output response $Y(j\omega)$; and (c) reactor impulse response $E(j\omega) = Y(j\omega)/X(j\omega)$.

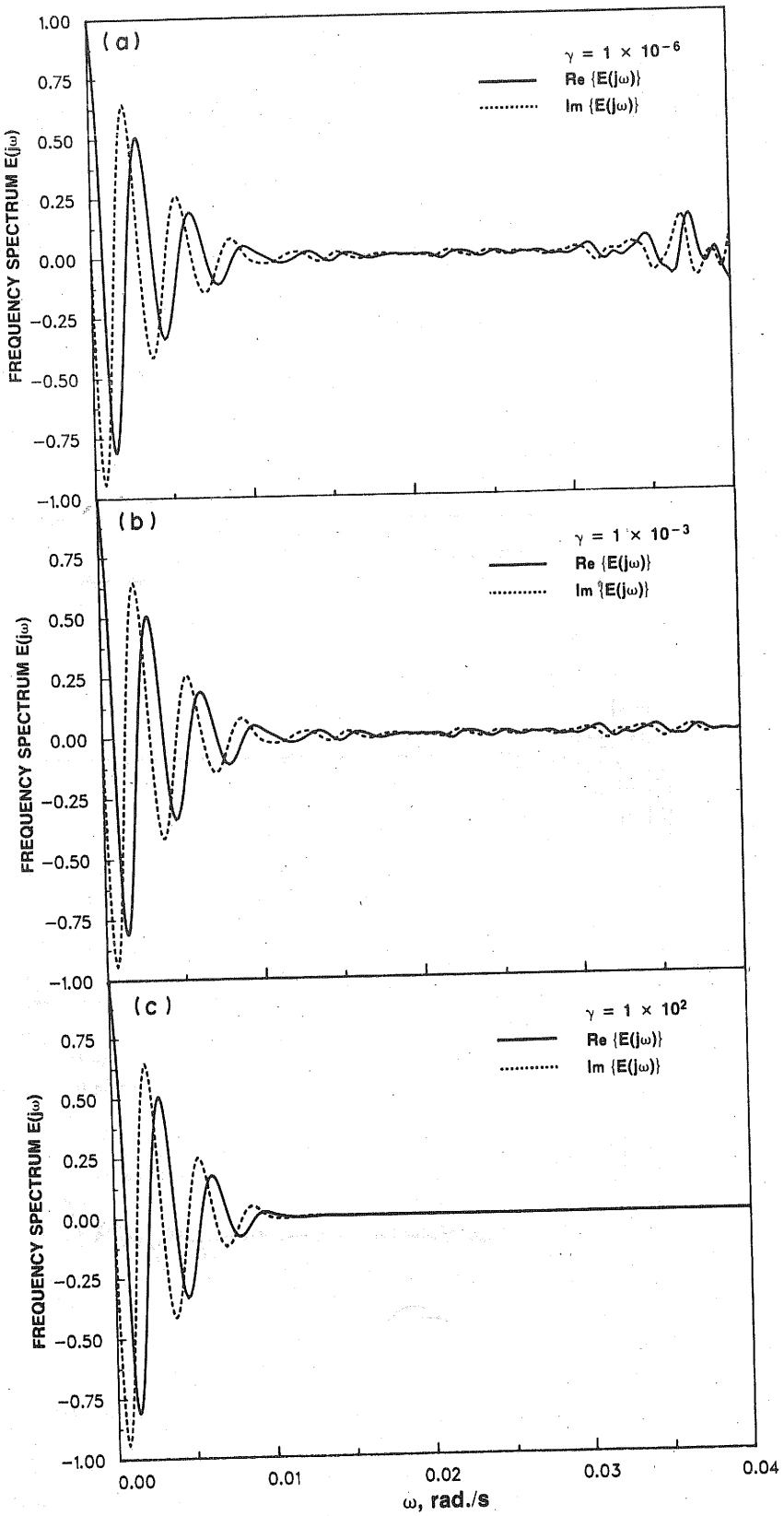

Fig. 4. Effect of the smoothing parameter γ on the Fourier-transform of the reactor impulse response obtained by deconvolution: (a) $\gamma = 10^{-6}$; (b) $\gamma = 10^{-3}$; and (c) $\gamma = 10^{2}$. Other parameters: $\Delta t = 2$ s, $N = 1024$, $T_s = N\Delta t = 2048$ s.

could not be distinguished when plotted. Increasing the smoothing parameter from 10^{-6} to 10^{2} results in the removal of the irregular oscillations in the Fourier-transform reactor impulse response, especially for $\omega \geqslant 0.015$. When compared to the reactor impulse response obtained without filtering (Fig. 3c), the results in Fig. 4 are quite significant in terms of demonstrating how the ill-effects of measurement errors and noise can be removed.

Another way of viewing the importance of using filtering when performing deconvolution is by examination of the reactor impulse response in the time-domain. Although a knowledge of the reactor impulse response in the Fourier transform as shown in Fig. 4 is quite useful, one objective of this work was to obtain the time-domain impulse response for subsequent applications, such as flow-model parameter estimation. Figures 5a–c show the results obtained when the Fourier-transformed reactor impulse responses given in Figs 4a–c are inverted to the time-domain using the inverse discrete Fourier transform via equation (10). Figure 5a shows that choosing $\gamma = 1 \times 10^{6}$ gives a time-domain response which shows some resemblance to a skewed pulse response peak, but otherwise contains many sharp spikes. Increasing γ by three orders-of-magnitude to $\gamma = 1 \times 10^{-3}$ as shown in Fig. 5b results in a substantial reduction of the spikes, but the overall quality is still not acceptable. Figure 5c shows that choosing $\gamma = 1 \times 10^{2}$ removes all of the remaining spikes from the impulse response so that a smooth curve is obtained.

As mentioned earlier, proper choice for the smoothing parameter γ will ensure that the reactor impulse response obtained by deconvolution of the input–output responses satisfies the convolution integral and other quantities related to it, for example the moment generating property. According to equation (11), the nth absolute moment of the reactor impulse response should be equal to the difference between the nth absolute moments of the normalized output and input responses. This latter criteria is tested in Figs 6a–c where the zeroth, first absolute and variance obtained from Figs 5a–c are plotted as a function of the smoothing parameter γ by following the procedure described after equation (12). Figure 6a shows that the zeroth moment has a constant value of $\mu_0 = 0.9984$ over the indicated range of γ, i.e. the area under $e_{a,j}$ vs t is nearly unity. This is in good agreement with the theoretical result that would be obtained if the tracer mass balance was satisfied. It suggests that the deconvolution procedure satisfies conservation of mass, at least over the indicated range of γ. The difference between the theoretical value and calculated value for the zeroth moment, i.e. $\epsilon = |1.0 - 0.9984| = 0.0016$, is within the numerical quadrature error of equation (12). Both the first absolute moment and variance, as shown by Figs 6b and c, respectively, remain constant with increasing values of γ until the range $\gamma = 10^{3}$–10^{3} is approached. For $\gamma \geqslant 10^{3}$, they either increase or decrease, neither of which is acceptable.

The above results suggest that evaluation of the moments of the reactor impulse response provide a fuzzy estimate of the upper limit on the value of the smoothing parameter, but no lower limit appears to emerge. This latter one can be estimated by inspection of the time-domain inverse at a series of γ values, such as those illustrated previously in Fig. 5. For the input–output data used in this example, a value of $\gamma = 1 \times 10^{2}$ removed the spurious noise from the impulse response, while providing moments that were in reasonable agreement with those obtained by differences from the output–input response curves.

Verification that the reactor impulse response obtained by the deconvolution procedure is acceptable is shown in Fig. 7a. Here, the normalized experimental output response y_j is compared to the output response obtained by convolution of the normalized experimental input response x_j with the reactor impulse response $e_{a,j}$. The agreement between the experimental output response and the calculated output response is excellent with a squared relative error of 0.35×10^{-2}. Figure 7b shows the results of the same operation, except that a smoothing parameter of $\gamma = 10^{6}$ has been used. This value of γ is clearly too large since the calculated output response underpredicts the experimental output response.

The reactor impulse response given in Fig. 5c can be used as the basis for parameter estimation in selected linear flow models. Here, the piston-diffusion-exchange or PDE model of Van Swaaij *et al.* (1969) is selected as the basis for obtaining model predictions. In Fig. 8, a sketch of the model is given along with the dimensionless forms of the tracer mass balance equations in both the mobile and stagnant phases. In this case, the stagnant phase refers to that portion of the reactor volume which is occupied by a stationary phase. This would include the catalyst packing and stagnant pockets of liquid that exist on the catalyst surfaces, such as at catalyst particle contact points. Definitions for the various quantities that appear in the equations are given in the Nomenclature. If tracer exchange between the mobile and stagnant phase is neglected, then the PDE model reduces to the piston-diffusion or PD model. Also, the number of unknown model parameters is reduced from four (Pe_L, τ, k and α) to two (Pe_L and τ). Closed-form expressions for the impulse responses of both models in the Laplace transform domain $\bar{E}(s, \bar{P})$ when Danckwerts boundary conditions are used can be readily developed by standard methods and are omitted here for brevity.

In Fig. 9 comparisons between the experimental tracer responses and the model predictions are given. Figure 9a shows the results obtained when the reactor impulse response $e_{a,j}$ determined by the deconvolution method using equations (9) and (10) is compared to the PD and PDE model prediction $e_{p,j}$ using equation (18). The model parameters indicated on the figure

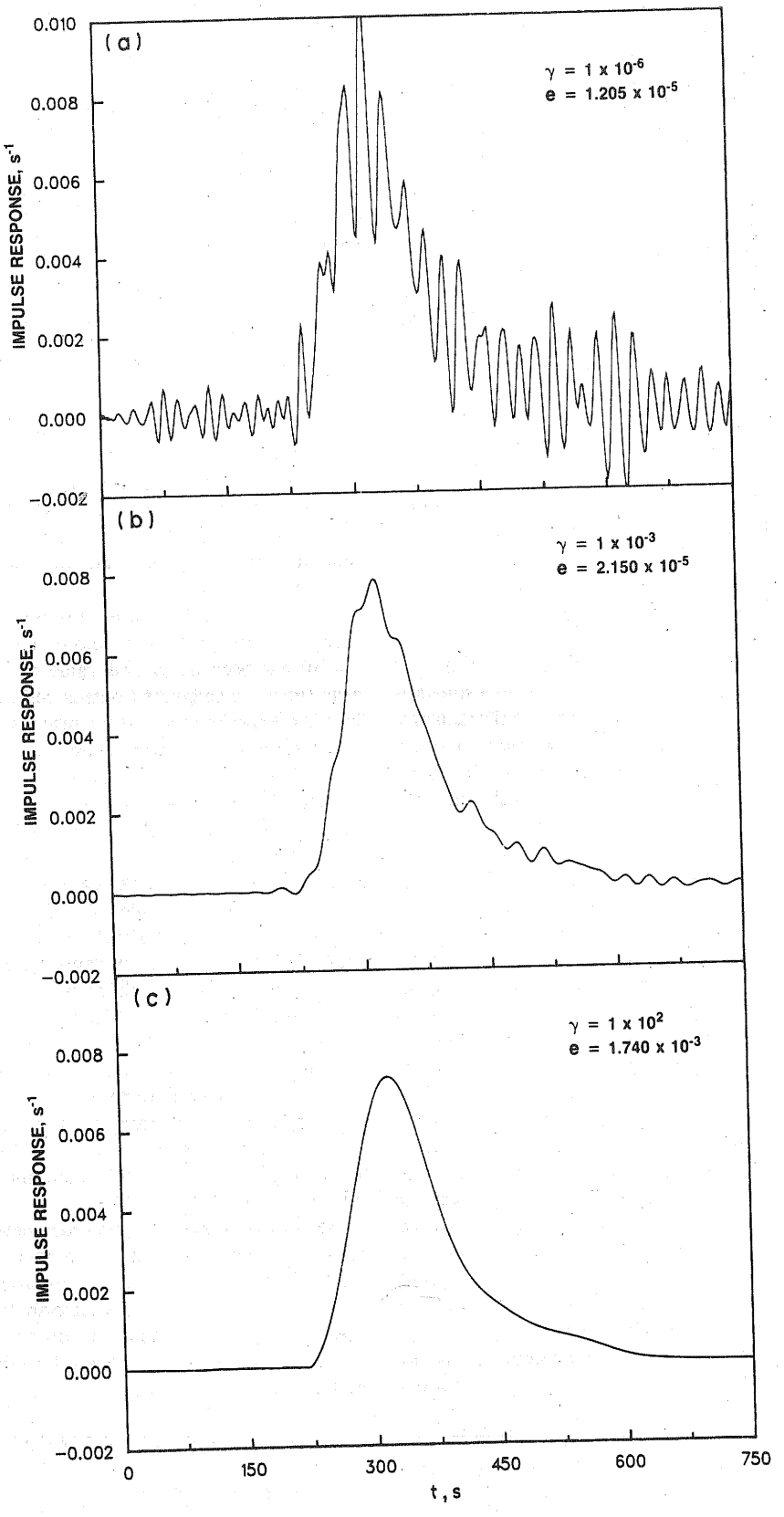

Fig. 5. Effect of the smoothing parameter γ on the time-domain reactor impulse obtained by deconvolution: (a) $\gamma = 10^{-6}$; (b) $\gamma = 10^{-3}$; and (c) $\gamma = 10^{2}$. Other parameters: $\Delta t = 2$ s, $N = 1024$, $T_s = N\,\Delta t = 2048$ s.

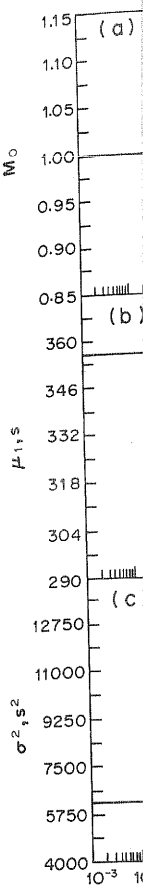

Fig. 6. Effect
moment, first
impulse respo

are based u
tion defined
Fig. 9a, ex
output resp
dicted outp
obtained by
tions (15) a
are based u
explained in

In terms
Fig. 9 show
ter PDE m
than the t
tional para
model, nam
parameter
phase exch
necessary t
sponse cur
mobile and
generally a
Sicardi *et*
data from
same mod

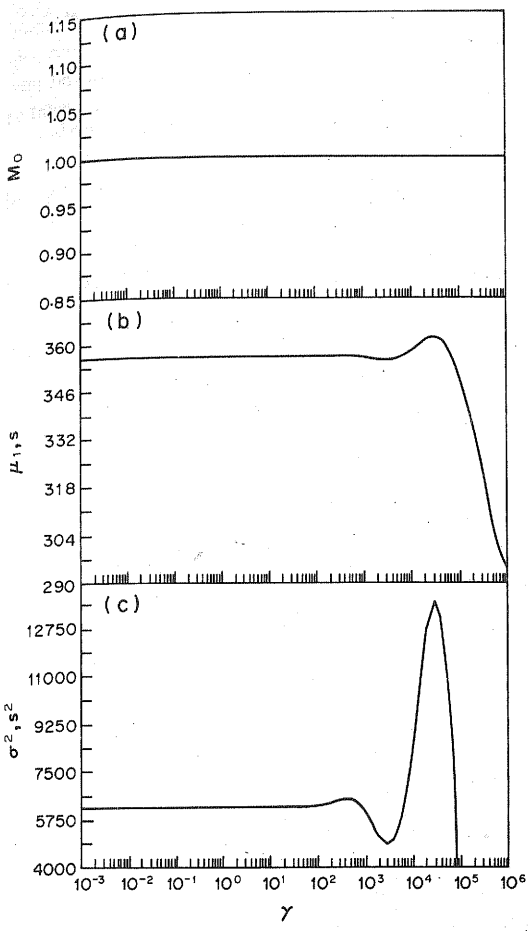

Fig. 6. Effect of the smoothing parameter γ on the zeroth moment, first absolute moment, and variance of the reactor impulse response: (a) M_0 vs γ; (b) μ_1 vs γ; and (c) σ^2 vs γ.

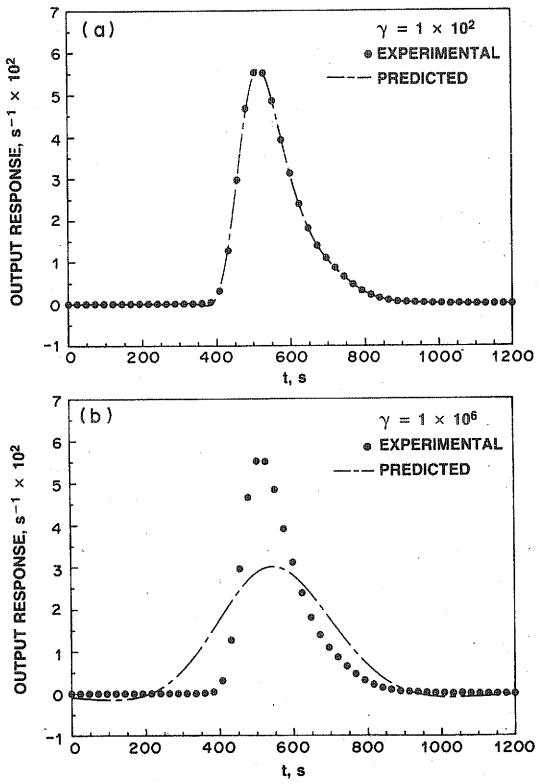

Fig. 7. Comparison of the normalized experimental system output response to the one obtained by convolution of $X(n)$ with $E(n)$ where the latter is derived from equation (9): (a) $\gamma = 10^2$; and (b) $\gamma = 10^6$. Other parameters: $\Delta t = 2$s, $N = 1024$, $T_s = N\Delta t = 2048$ s.

are based upon minimization of the objective function defined by equation (17). Figure 9b is similar to Fig. 9a, except that the normalized experimental output response y_j is compared to the model-predicted output response $y_{p,j}$ where the latter one is obtained by the convolution approach using equations (15) and (16). Here, the indicated parameters are based upon the minimization of equation (21) as explained in more detail in a previous section.

In terms of model discrimination, inspection of Fig. 9 shows that the predictions of the four-parameter PDE model are in better agreement with the data than the two-parameter PD model. The two additional parameters that are incorporated into the PDE model, namely the stagnant-to-mobile phase holdup parameter $\alpha = H_s/H_m$ and the mobile-to-stagnant phase exchange coefficient $k = k_m a$, appear to be necessary to accurately describe the tail of the response curves where tracer diffusion between the mobile and stagnant phases is most pronounced. This generally agrees with the independent observations of Sicardi *et al.* (1980) who interpreted step-response data from a laboratory trickle-bed reactor using the same model.

It is worth noting that in the work of Sicardi *et al.* (1980), the step input was assumed to be an ideal one since $x(t) = H(t)$ was used as the normalized forcing function where $H(t)$ denotes the Heaviside step function. Parameter estimation was then performed by minimization of an objective function whose form was identical to equation (21) which is based upon matching the model-predicted and experimental output responses. It is impossible to assess whether the final values for the parameters were affected by the use of an ideal step vs a nonideal step as forcing functions since this comparison was not made.

PISTON-DIFFUSION-EXCHANGE (P.D.E.) MODEL

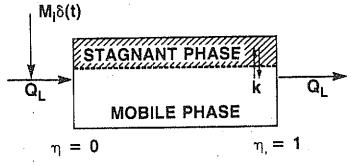

$$\tau \frac{\partial \theta_L}{\partial t} = \frac{1}{Pe_L} \frac{\partial^2 \theta_L}{\partial \eta^2} - \frac{\partial \theta_L}{\partial \eta} - k\tau(\alpha + 1)(\theta_L - \theta_S)$$

$$\tau\alpha \frac{\partial \theta_S}{\partial t} = k\tau(\alpha + 1)(\theta_L - \theta_S)$$

Fig. 8. Illustration of the piston-diffusion-exchange model for tracer transport in a packed-bed and the governing tracer mass balance equations.

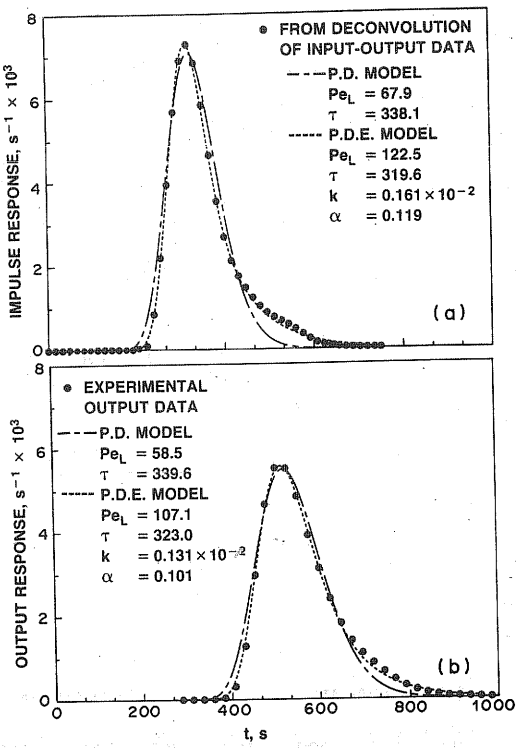

Fig. 9. Comparison of the piston-diffusion and piston-diffusion-exchange model predictions with the normalized tracer responses: (a) comparison of the reactor impulse response obtained by deconvolution with the model-predicted impulse response; and (b) comparison of the normalized experimental output response with the model-predicted output response obtained by convolution.

An important issue that arises is whether or not the model parameters obtained by time-domain parameter estimation using the deconvoluted reactor impulse response agree with those obtained from the convolution method. Although the methods differ in their approach, they should, in principle, lead to identical values for the model parameters since both are directly related through the convolution integral. The PD model results are not included in this discussion since, as mentioned above, it fails to accurately represent the experimental data when compared to the PDE model.

In Table 1, a comparison of the PDE model parameters obtained from both methods is given in terms of both absolute differences, and percentage relative differences. Since convolution is a well-posed operation when compared to deconvolution, the convolution-based parameters were selected as the normalizing factor when evaluating the relative differences. Inspection of the relative differences shows that they collectively range from 1 to about 24%. The mean residence time of the external liquid τ and the ratio of liquid holdups α, which are parameters that depend upon the first moment of the PDE model impulse response (Van Swaaij *et al.*, 1969), have relative differences of 1 and 18%, respectively. The Peclet number of the mobile phase Pe_L and the dimensionless exchange coefficient k, which depend upon the variance and skewness of the impulse response, have relative differences of nearly 18 and 24%, respectively. These results suggest that parameters associated with the curve moments which are greater than unity have the greatest errors, since slight differences in the tailing of the response curves have the greatest influence in estimating higher order moments (Duduković, 1986; Nauman and Buffham, 1983; Ramachandran and Chaudhari, 1983).

To assess parametric sensitivity, some additional comparisons were made. The parameters given in Fig. 9b, obtained via parameter estimation using the normalized tracer output response data by the convolution method, were first used to obtain a PDE model-predicted impulse response. This impulse response was then compared to the one obtained by deconvolution of the input–output response data, as shown in the smooth curve in Fig. 5c or the points on Fig. 9a. To investigate the reverse situation, the parameters given in Fig. 9a, corresponding to those obtained by fitting the deconvolution impulse response to the PDE model impulse response, were used to obtain a PDE model-predicted output response. This output response was then compared to the one shown in Fig. 9b.

The results of the above exercise are shown in Fig. 10. The dashed lines in both figures show the PDE model predictions when parameter estimation is performed in the usual fashion as described above and shown earlier by the dashed lines of Fig. 9. The solid lines show the results obtained when the parameters obtained from deconvolution are used to obtain model-predictions for convolution and *vice versa*. The differences between the model-predicted responses obtained by these two methods are very

Table 1. Comparison of PDE model parameters obtained by convolution and deconvolution

Parameter	Convolution method	Deconvolution method	Absolute difference[1]	Relative error (%)[2]
τ	323.0	319.6	3.4	1.05
μ	0.101	0.119	0.018	17.82
Pe_L	107.1	122.5	15.4	14.38
k	0.130×10^{-2}	0.161×10^{-2}	3.1×10^{-4}	23.85

[1]Defined as |parameter value (convolution method) − parameter value (deconvolution method)|.

[2]Defined as $\dfrac{|\text{parameter value (convolution method)} - \text{parameter value (deconvolution method)}|}{\text{Parameter value (convolution method)}} \times 100.$

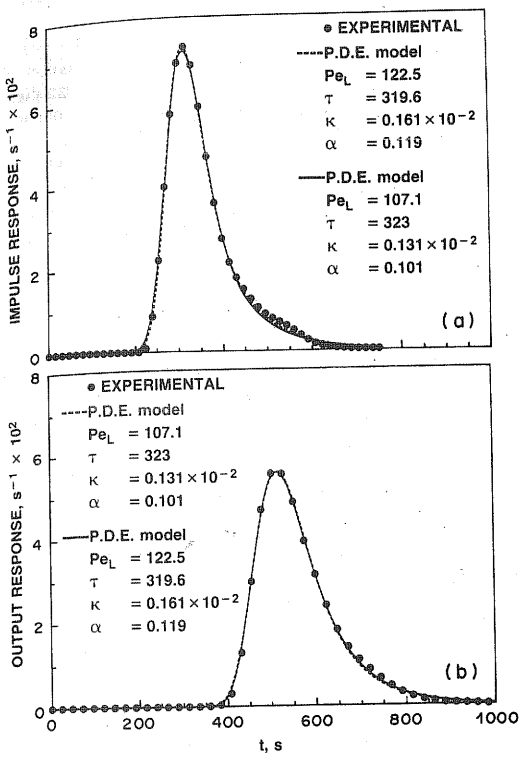

Fig. 10. Comparison of the normalized tracer response data to the PDE model predictions: (a) comparison of impulse responses; and (b) comparison of output responses.

slight, but they can be seen in the initial part and the tail of the response curve. These differences, however, are within the accuracy of the experimental tracer response measurements so that both sets of parameters listed in Table 1 are acceptable. Confidence limits on the parameters can only be assigned when data from repeated experiments is available for proper statistical error analysis. This is complicated enough to be considered as a topic for a possible future study.

SUMMARY AND CLOSING REMARKS

Two methods have been presented for analysis of nonideal pulse tracer response data that use the discrete form of the convolution integral as the basis. In both cases, it was assumed that experimental input–output tracer data were available that represented real-world transient response measurements for a particular system. For situations where the input response could not be readily obtained, such as in large-scale commercial reactor systems, an appropriate flow model that provides a reasonable description of the tracer transport in the injection-sampling system could be incorporated.

The first method used the principle of deconvolution to obtain the impulse response of the test section from the given discrete data sequences of the input $X(j\Delta t)$ and the output $Y(j\Delta t)$. It was pointed out that application of standard matrix methods cannot be used for most problems of practical interest since the data record lengths are too large for most computers, and the inverse operator is ill-defined. It was also shown that standard Fourier transform methods also fail since measurement errors and noise in the data give an apparent impulse response that is dominated by the noise.

To overcome the above problems associated with the standard methods, a method for performing deconvolution based upon regularization was introduced. Expressions derived from this method which yield the impulse response in both the Fourier transform and time-domain were set forth, and their implementation was summarized. Techniques based upon the method of moments and convolution principles were presented for identifying reasonable estimates of the regularization parameter. Up until now, these had not been demonstrated on real data so that previous attempts at selecting this parameter were somewhat arbitrary. Graphical inspection of the impulse response at a series of regularization parameter values as well as utilization of the above-stated methods is recommended to ensure validity of the results.

The second method for interpretation of nonideal pulse tracer responses was based upon discrete convolution of the input response with an assumed linear flow model to produce a model-predicted output response. By performing the convolution using the discrete Fourier transform, the output response in the time-domain could be readily evaluated by the inverse operation. Comparison of this latter output response to the normalized experimental output allowed the model parameters to be obtained by parameter estimation methods. This approach of performing the convolution operation in the Fourier transform domain followed by inversion to the time-domain using the fast Fourier transform avoids the direct matrix evaluation of the convolution integral. This latter operation, as in the case of matrix deconvolution, cannot be performed on most computers for most practical input–output tracer response data sets due to excessive matrix storage requirements. Unlike the case of deconvolution, however, the convolution operation is well-posed so that the presence of measurements errors and noise in the data does not introduce spurious solution behavior.

Both the convolution and deconvolution methods described here can be viewed as more advanced techniques for analysis of tracer response data than previous ones, for example, the popular method of moments. If the ultimate goal is to discriminate between various linear tracer flow models and to perform parameter estimation, then the convolution method is recommended since it is the easiest to apply. If, for example, the various experimental tracer age functions for the test section are desired for some subsequent purpose, then deconvolution of the input–output data to obtain the impulse response is essential.

NOMENCLATURE

a = Interfacial area for mass transfer of the tracer between the mobile and stagnant phases per unit volume of the combined mobile and stagnant phases, cm^{-1}

a_j = Sampled value of a time domain complex function $a_p(t)$ appearing in equation (5)

a_m = Interfacial area for mass transfer of the tracer between the mobile and stagnant phases per unit volume of the mobile phase, $a(1+\alpha)$, cm^{-1}

$A(n)$ = Sampled value of the discrete Fourier transform a_j defined by equation (5)

b = Real part of the Laplace transform variables defined by equation (20)

$B(n)$ = Sampled value of the discrete Fourier transform of the noise sequence ϵ_k appearing in equation (6)

c_j = Sampled value of the smoothing formula coefficients first appearing after equation (9)

$C(n)$ = Sampled value of the discrete Fourier transform of the c_j first appearing in equation (9)

$C^*(n)$ = Complex conjugate of $C(n)$ appearing in equation (9)

$\mathbb{C}$ = Matrix that contains the smoothing formula coefficients first appearing in equation (7)

$C_{L0}(t)$ = Concentration of tracer in the mobile phase at the reactor inlet, $(M_i/Q_L)\delta(t)$, mol cm^{-3} of mobile phase

C_m = Concentration of tracer in the mobile phase, mol cm^{-3} of mobile phase

C_s = Concentration of tracer in the stagnant phase, mol cm^{-3} of stagnant phase

D_{L0} = Axial dispersion coefficient of the mobile phase based on the reactor cross-sectional area, cm^2s^{-1}

e_j = Sampled value of the exact time-domain impulse response first appearing in equation (1)

$\bar{e}$ = Column matrix whose elements are the e_j first appearing in equation (3)

$E(n)$ = Sampled value of the discrete Fourier transform of e_j defined by equation (6)

$e_{a,j}$ = Sampled value of the approximate time-domain impulse response defined by equation (10)

$\bar{e}_a$ = Column matrix whose elements are the $e_{a,j}$ first appearing in equation (7)

$E_a(n)$ = Sampled value of the discrete Fourier transform of $e_{a,j}$ defined by equation (9)

$e_{p,j}$ = Sampled value of the model-predicted impulse response defined by equation (18)

$\bar{E}(s, \bar{P})$ = Closed-form expression for the model-predicted Laplace transformed impulse response first appearing above equation (15)

$\bar{E}(n, \bar{P})$ = Sampled value of the discrete Fourier transform of $\bar{E}(s, \bar{P})$ appearing in equation (15)

$\bar{E}_i$ = Imaginary part of $\bar{E}(s, \bar{P})$ appearing after equation (15)

$\bar{E}_r$ = Real part of $\bar{E}(s, \bar{P})$ appearing after equation (15)

E_r = Rounding error appearing in equation (20)

$E(t, \bar{P})$ = Closed-form expression for the model-predicted impulse response in the time-domain, s^{-1}

$E(t)$ = Continuous form of the normalized impulse response, s^{-1}

H_m = Holdup of the mobile phase, cm^3 of mobile phase cm^{-3} of reactor

H_s = Holdup of the stagnant phase, cm^3 of stagnant phase cm^{-3} of reactor

$i = \sqrt{-1}$

j = Summation index

k = Volumetric mass transfer coefficient for transport of the tracer between the mobile and stagnant phases, $k_m a$, s^{-1}

k_m = Mass transfer coefficient for transport of the tracer between the mobile and stagnant phases, s^{-1}

L = Reactor length, cm

M = Constant appearing in equation (19)

MSE = Mean-squared error defined by equation (14)

n = Index used to denote a particular sample, or variable used to denote the order of a particular response curve moment

N = Total number of points, or total number of sampled function values

$\bar{P}$ = Column matrix of model parameter values

Pe_L = Peclet number of the mobile phase, Lu_{sm}/D_{L0}, dimensionless

Q_L = Volumetric flowrate of the mobile phase, cm^3s^{-1}

$\bar{r}$ = Column vector of residual values appearing above equation (7)

s = Laplace transform variable, s^{-1}

t = time, s

T = Sampling time period, $N\Delta t$, s

u_{sm} = Superficial velocity of the mobile phase, cm s^{-1}

w_j = Weights assigned to sample j first appearing in equation (17)

x_j = Sampled value of the normalized experimental system input response, $X(j\,\Delta t)/(M_i/Q_L)$, s^{-1}

$\mathbb{x}$ = Matrix whose elements are the x_j first appearing in equation (3)

$X(j\Delta t)$ = Sampled value of the system input response measured by the detector before normalization, arbitrary units

$x(t)$ = Continuous form of the normalized input response, s^{-1}

$X(n)$ = Sampled value of the discrete Fourier transform of x_j first appearing in equation (6)

$X^*(n)$ = Complex conjugate of $X(n)$ appearing in equation (9)

y_j = Sampled value of the normalized experimental system output response, $Y(j\Delta t)/(M_i/Q_L)$, s^{-1}

$\bar{y}$ = Column matrix whose elements are the y_j defined by equation (3)

$Y(j\Delta t)$ = Sampled value of the system output response measured by the detector before normalization, arbitrary units

$Y(n)$ = Sampled value of the discrete Fourier transform of y_j first appearing in equation (6)

$Y^*(n)$ = Complex conjugate of $Y(n)$ appearing in equation (14)

$y(t)$ = Continuous form of the normalized output response, s^{-1}

$Y_p(n, \bar{P})$ = Sampled value of the discrete Fourier transform of the model-predicted output response defined by equation (15)

$Y_{p,j}$ = Sampled value of the model-predicted output response defined by equation (16)

z_j = Sampled value of the normalized error-free output response appearing in equation (1)

$Z(n)$ = Sampled value of the discrete Fourier transform of z_j appearing in equation (6)

Greek

α = Ratio of stagnant phase to mobile phase fluid holdups, H_s/H_m, cm^3 of stagnant phase cm^{-3} of mobile phase

γ = Smoothing parameter first appearing in equation (7)

$\delta(t)$ = Dirac delta function, s^{-1}

ϵ_k = Difference between the experimental value of the normalized output response and the exact value defined by equation (1), s^{-1}

η = Reactor axial distance, z/L, dimensionless

$\mu_{n,r}$ = nth absolute moment of the reactor impulse response, s^n

$\mu'_{n,r}$ = nth absolute moment of the reactor impulse response calculated from the deconvolution method, s^n

$\mu_{n,v}$ = nth absolute moment of the input response, s^n

$\mu_{n,r}$ = nth absolute moment of the input response, s^n
θ_L = Concentration of tracer in the mobile phase, $C_m/C_{LO}(t)$, dimensionless
θ_S = Concentration of tracer in the stagnant phase, $C_s/C_{LO}(t)$, dimensionless
τ = Mean residence time of tracer in the mobile phase, LH_m/u_{sm}, s
ϕ = Regularization objective function defined by equation (7)
ϕ_c = Objective function used for parameter estimation by the convolution method defined by equation (21)
ϕ_d = Objective function used for parameter estimation by the deconvolution method defined by equation (17)
ω_n = Frequency value, $2\pi n/T$, rad s^{-1}

REFERENCES

Anderssen A. S. and E. T. White, Parameter estimation by the transfer function method. *Chem. Engng Sci.* **25,** 1015–1021 (1970).

Anderssen A. S. and E. T. White, Parameter estimation by the weighted moments method. *Chem. Engng Sci.* **26,** 1203–1221 (1977).

Aris R., Notes on the diffusion type model for longitudinal mixing in flow. *Chem. Engng Sci.* **9,** 266–267 (1959).

Baker C. T. H., *The Numerical Treatment of Integral Equations*. Clarendon Press, Oxford (1977).

Bischoff K. B., Notes on the diffusion-type model for longitudinal mixing in flow. *Chem. Engng Sci.* **12,** 69–70 (1960).

Blass W. E. and G. W. Halsey, *Deconvolution of Absorption Spectra*. Academic Press, New York (1981).

Boersma-Klein W. and J. A. Moulijn, The evaluation in time domain of mass transfer parameters from chromatographic peaks. *Chem. Engng Sci.* **34,** 959–969 (1979).

Brigham E. O., *The Fast Fourier Transform*. Prentice-Hall, Englewood Cliffs, New Jersey (1974).

Chou T. S. and L. L. Hegedus, Transient diffusivity measurements in catalyst pellets with two zones of differing diffusivities. Report GMR-2474, General Motors Research Laboratories (1977).

Clements W. C. Jr, A note on the determination of the parameters of the longitudinal dispersion model from experimental data. *Chem. Engng Sci.* **24,** 957–963 (1969).

Colombo A. J., G. Baldi and S. Sicardi, Solid–liquid contacting effectiveness in trickle-bed reactors. *Chem. Engng Sci.* **31,** 1101–1108 (1976).

Crump K. S., Numerical inversion of Laplace transforms using a Fourier series approximation. *J. ACM* **23,** 89–96 (1976).

de Hoog F. R., Review of Fredholm integral equations of the first kind. In *The Application and Numerical Solution of Integral Equations* (R. S. Anderssen, F. R. de Hoog and M. A. Lukas, Eds), pp. 235–255. Sijthoff & Noordhoff, The Netherlands (1980).

Dogu T., Extension of moment analysis to nonlinear systems. *AIChE Jl* **32,** 849–852 (1986).

Dogu G. and J. M. Smith, A dynamic method for catalyst diffusivities. *AIChE Jl* **21,** 58–61 (1975).

Dogu T., A. Keskin, G. Dogu and J. M. Smith, Single-pellet moment method for analysis of gas–solid reactions. *AIChE Jl* **32,** 743–750 (1986).

Duduković M. P., Tracer methods in chemical reactors. Techniques and applications. In *Chemical Reactor Design and Technology* (H. I. deLasa, Ed.). *NATO Advanced Science Institutes Series E,* **110,** 107–189. Martinus Nijhoff, The Netherlands (1986).

Eroglu I. and T. Dogu, Dynamic analysis of a trickle-bed reactor by moment technique. *Chem. Engng Sci.* **38,** 801–815 (1983).

Fahim M. A. and N. Wakao, Parameter estimation from tracer response measurements. *Chem. Engng Jl* **25,** 1–8 (1982).

Felder R. M., R. E. Harrison and R. W. Rousseau, Parameter estimation by curve fitting techniques and the method of moments. *Chem. Engng Commun.* **1,** 187–189 (1974).

Fu B. S. J., Tracer analysis of recirculating systems. Ph.D. Thesis, Illinois Institute of Technology, Chicago (1970).

Furusawa T. and J. M. Smith, Fluid particle and intraparticle mass transport rates in slurries. *Ind. Engng Chem. Fundam.* **12,** 197–203 (1973a).

Furusawa T. and J. M. Smith, Mass transport rates in slurries by chromatography. *Ind. Engng Chem. Fundam.* **12,** 360–364 (1973b).

Furusawa T. and J. M. Smith, Intraparticle mass transport in slurries by dynamic adsorption studies. *AIChE Jl* **20,** 88–93 (1974).

Furusawa T. and M. Suzuki, Moment analysis of concentration decay in a batch adsorption vessel. *J. Chem. Engng Japan* **8,** 119–122 (1975).

Furusawa T., M. Suzuki and J. M. Smith, Rate parameters in heterogeneous catalysis by pulse techniques. *Catal. Rev. Sci. Engng* **13,** 43–76 (1976).

Gangwal S. K., R. R. Hudgins, A. W. Bryson and P. L. Silveston, Interpretation of chromatographic peaks by Fourier analysis. *Can. Jl Chem. Engng* **49,** 113–119 (1971).

Gosset R., Parameter estimation in dynamic responses of linear systems. *Proc. Third Symp. Use of Computers in Chemical Engineering*, pp. 386–397, GLIWICE (1974).

Harrison R. E., R. M. Felder and R. W. Rousseau, Accuracy of parameter estimation by frequency response analysis. *Ind. Engng Chem., Process Des. Dev.* **13,** 389–391 (1974).

Haynes H. W. Jr, Mass transport characteristics of zeolite cracking catalysts. U.S. Dept of Energy Quarterly Report (1978).

Haynes H. W. Jr, Private Communication (1986).

Hays J. R., W. C. Clements Jr and T. R. Harris, The frequency domain evaluation of mathematical models for dynamic systems. *AIChE Jl* **13,** 374–378 (1967).

Hunt B. R., The inverse problem of radiography. *Math. Biosci.* **8,** 161–179 (1970).

Hunt B. R., Biased estimation for nonparametric identification of linear systems. *Math. Biosci.* **10,** 215–237 (1971).

IMSL, *Mathematical Library Reference Manual*, Edn 9, Houston (1982).

Jakeman A. J. and P. Young, Systems identification and estimation for convolution integral equations. In *The Application and Numerical Solution of Integral Equations* (R. S. Anderssen, F. R. de Hoog and M. A. Lukas, Eds) pp. 235–255, Sijthoff & Noordhoff, The Netherlands (1980).

Jansson P. A. (Ed.), *Deconvolution With Applications in Spectroscopy*. Academic Press, Orlando (1984).

Kan K. M. and P. F. Greenfield, A residence time model for trickle-flow reactors incorporating incomplete mixing in stagnant regions. *AIChE Jl* **29,** 123–130 (1983).

Kobayashi H. and M. Kobayashi, Transient response method in heterogeneous catalysis. *Cat. Rev.-Sci. Engng* **10,** 139–176 (1974).

Lee D., S. Kaguei and N. Wakao, Relation between adsorption equilibrium constant, fluid dispersion coefficient and intraparticle effective diffusivity in time-domain analysis of adsorption chromatography curves. *J. Chem. Engng Japan* **14,** 161–163 (1981).

Levenspiel O., *Chemical Reaction Engineering*. Wiley, New York (1972).

Michelsen M. L., A least-squares method for residence time distribution analysis. *Chem. Engng Jl* **4,** 171–179 (1972).

Michelsen M. L. and K. Ostergaard, The use of residence time distribution data for estimation of parameters in the

axial dispersion model. *Chem. Engng Sci.* **25,** 583–592 (1970).
Mills P. L. and M. P. Duduković, Evaluation of liquid–solid contacting in trickle-bed reactors by tracer methods. *AIChE Jl* **27,** 893–904 (1981).
Mills P. L., W. P. Wu and M. P. Duduković, Tracer analysis in systems with two-phase flow. *AIChE Jl* **25,** 885–890 (1979).
Mixon F. O., D. R. Whitaker and J. C. Orcutt, Axial dispersion and heat transfer in liquid–liquid spray towers. *AIChE Jl* **13,** 21–28 (1967).
Nauman E. B. and B. A. Buffham, *Mixing in Continuous Flow Systems*. Wiley, New York (1983).
Niyama H. and J. M. Smith, Adsorption of nitric oxide in aqueous slurries of activated carbon. Transport rates by moment analysis of dynamic data. *AIChE Jl* **22,** 961–970 (1976).
Ostergaard K. and M. L. Michelsen, On the use of an imperfect tracer pulse method for determination of hold-up and axial mixing. *Can. J. Chem. Engng* **47,** 107–112 (1969).
Pamuk I. and T. Dogu, A moment method for the analysis of a two-phase model for fluidized beds. *Chem. Engng J.* **16,** 11–18 (1978).
Pehtö A. and R. D. Noble (Eds), *Residence Time Distribution Theory in Chemical Engineering*. Weinheim, Verlag-Chemie (1982).
Phillips D., A technique for the numerical solution of certain integral equations of the first kind. *Jl. Ass. Comput. Mach.* **9,** 97–101 (1962).
Radeke K. H., Critical remarks on using moments method. *Ind. Engng Chem. Fundam.* **28,** 302–303 (1981).
Rajakumar A. and P. R. Krishnaswamy, Time to frequency conversion of step response data. *Ind. Engng Chem., Process Des. Dev.* **14,** 250–255 (1975).
Ramachandran P. A. and R. V. Chaudhari, *Three-Phase Catalytic Reactors*, Chap. 5. Gordon & Breach, London (1983).
Ramachandran P. A. and J. M. Smith, Dynamics of three-phase slurry reactors. *Chem. Engng Sci.* **32,** 873–880 (1977).
Ramachandran P. A. and J. M. Smith, Adsorption of hydrogen sulfide in a slurry reactor. *Ind. Engng Chem. Fundam.* **17,** 17–23 (1978a).
Ramachandran P. A. and J. M. Smith, Transport rates by moment analysis of dynamic data. *Ind. Engng Chem. Fundam.* **17,** 148–160 (1978b).
Ramachandran P. A. and J. M. Smith, Dynamic behavior of trickle-bed reactors. *Chem. Engng Sci.* **34,** 75–91 (1979).
Ramachandran P. A., M. P. Duduković and P. L. Mills, A new model for assessment of external liquid–solid contacting in trickle-bed reactors by tracer response measurements. *Chem. Engng Sci.* **41,** 855–860 (1986).
Schneider P. and J. M. Smith, Adsorption rate constants from chromatography. *AIChE Jl* **14,** 762–771 (1968a).
Schneider P. and J. M. Smith, Chromatographic study of surface diffusion. *AIChE Jl* **14,** 886–895 (1968b).
Schwartz J. G., E. Weger and M. P. Duduković, A new tracer method for determination of liquid–solid contacting efficiency in trickle-bed reactors. *AIChE Jl* **22,** 894–904 (1976).
Seinfeld J. H. and L. Lapidus, *Mathematical Methods in Chemical Engineering, Vol. 3, Process Modeling, Estimation and Identification*, Chap. 7. Prentice-Hall, Englewood Cliffs, New Jersey (1974).
Shinnar R., Chemical reactor modeling—the desirable and the achievable. In *Chemical Reaction Engineering Reviews—Houston* (D. Luss and V. W. Weekman Jr, Eds), *ACS Symp. Ser.* **72,** 1–36 (1978).
Sicardi S., G. Baldi and V. Specchia, Hydrodynamic models for the interpretation of the liquid flow in trickle-bed reactors. *Chem. Engng Sci.* **35,** 1775–1782 (1980).
Suzuki M. and J. M. Smith, Kinetic studies by chromatography. *Chem. Engng Sci.* **26,** 221–235 (1971).
Twomey S., The application of numerical filtering to the solution of integral equations encountered in indirect sensing measurements. *J. Franklin Inst.* **279,** 95–109 (1965).
Van Swaaij W. P. M., J. C. Charpentier and J. Villermaux, Residence time distribution in the liquid phase of trickle flow in packed columns. *Chem. Engng Sci.* **24,** 1083–1095 (1969).
Van Zee G. A., W. M. M. Schinkel and O. H. Bosgra, Estimation of the transfer function, time moments, and model parameters of a flow process. *AIChE Jl* **33,** 341–346 (1987).
Wakao N. and K. Tanaka, Comparison of moment method and Fourier analysis in chromatograph. *J. Chem. Engng Japan* **6,** 338–342 (1973).
Wakao N., S. Kaguei and J. M. Smith, Parameter estimation in adsorption chromatography by real-time analysis. *J. Chem. Engng Japan* **12,** 481–483 (1978).
Wakao N., S. Kaguei and J. M. Smith, Adsorption chromatography measurements. Parameter determination. *Ind. Engng Chem. Fundam.* **19,** 363–367 (1980).
Waldram S. P., P. L. Mills and M. P. Duduković, Determination of binary gas diffusion coefficients by steady and unsteady-state analysis of single pellet reactor data. *Math. Comput. Model.* **11,** 38–42 (1988).
Watanabe K. and D. M. Himmelblau, Detection and location of a leak in a gas-transport pipeline by a new acoustic method. *AIChE Jl* **32,** 1690–1701 (1986).
Weinstein H. and M. P. Duduković, Tracer methods in the circulation. In *Topics in Transport Phenomena* (C. Gutfinger, Ed.), pp. 345–453. Hemisphere, New York (1975).
Wen C. Y. and L. T. Fan, *Models For Flow Systems and Chemical Reactors*. Marcel-Dekker, New York (1975).
Wolff H. J., K. H. Radeke and D. Gelbin, Heat and mass transfer in packed-beds—IV. Use of weighted moments to determine axial dispersion coefficients. *Chem. Engng Sci.* **34,** 101–107 (1979).
Wolff H. J., K. H. Radeke and D. Gelbin, Weighted moments and the pore diffusion model. *Chem. Engng Sci.* **35,** 1481–1485 (1980).
Ziolkowski A., *Deconvolution*. International Human Resources Development Corporation, Boston (1984).